

Image resonance in the many-body density of states at a metal surface

G. Fratesi* and G. P. Brivio

*INFN and Dipartimento di Scienza dei Materiali,
Università di Milano-Bicocca, via Cozzi 53, 20125 Milano, Italy*

Patrick Rinke† and R. W. Godby

Department of Physics, University of York, York YO10 5DD, United Kingdom

(Dated: November 20, 2018)

The electronic properties of a semi-infinite metal surface without a bulk gap are studied by a formalism able to account for the continuous spectrum of the system. The density of states at the surface is calculated within the *GW* approximation of many-body perturbation theory. We demonstrate the presence of an unoccupied surface resonance peaked at the position of the first image state. The resonance encompasses the whole Rydberg series of image states and cannot be resolved into individual peaks. Its origin is the shift in spectral weight when many-body correlation effects are taken into account.

PACS numbers: 73.20.At

I. INTRODUCTION

For the understanding of several fundamental properties of condensed matter surfaces, the knowledge of the electronic density of states and of the parallel-wavevector-resolved density are essential. The dispersion of both occupied and excited surface states, the influence of the changes of the electronic structure in thin film growth and enhanced magnetism are just a few examples of relevant quantities. Experimentally the density of states can be probed by a variety of techniques such as photoemission spectroscopies¹ (angle resolved, integrated, inverse and two-photon), and scanning tunneling microscopy.² To provide an adequate theoretical description of the experimental observables, it is necessary to employ methods which retain the continuous character of the spectrum. In other words one has to take into account that certain quantities may be defined for any energy in a given energy interval. Furthermore, the formalism must be capable of describing excited-state properties.

Regarding excited states, considerable experimental interest has been devoted to image-potential induced (IPI) states^{3,4,5,6} and resonances.^{7,8,9,10} IPI states are present in systems where a bulk band gap provides a barrier, trapping electrons in the image tail of the surface potential. If no gap is present at the IPI energies, an electron is not reflected completely at the bulk barrier and hybridization with surface truncated bulk states becomes possible. This results in the formation of resonances for some materials. A comprehensive theoretical description of IPI states has been given by Echenique and coworkers,^{11,12,13,14} whereas the situation for IPI resonances is much less satisfactory. In principle, IPI resonances are intrinsically contained in the many-body framework, already at the level of the *GW* approximation,¹⁵ but to our knowledge surfaces have only been investigated in this context using a repeated slab geometry.^{16,17,18} Such a simplified treatment cannot capture the continuous spectrum of a real surface, be-

cause the spectral function will inevitably be composed of a limited number of sharp, discrete peaks in place of the resonance.

In this Article we present *ab initio* many-body calculations of the local density of states (LDOS) of a semi-infinite jellium surface and demonstrate the presence of a broad IPI resonance. We calculate the LDOS – in its many-body generalization, the spectral function¹⁵ – decomposed according to the surface parallel wave-vector \mathbf{k}_{\parallel} within the surface *xy*-plane as

$$\sigma(\mathbf{r}, \omega) = \int \frac{d^2\mathbf{k}_{\parallel}}{(2\pi)^2} A(z, \mathbf{k}_{\parallel}, \omega), \quad (1)$$

where A is the \mathbf{k}_{\parallel} -resolved LDOS or spectral weight function, defined by

$$A(z, \mathbf{k}_{\parallel}, \omega) = -\frac{1}{\pi} \Im G(z, z, \mathbf{k}_{\parallel}, \omega) \text{sgn}(\omega - \mu). \quad (2)$$

Here G is the one-particle Green's function in the representation indicated, and Hartree atomic units ($a_0 = 0.529 \text{ \AA}$, 1 hartree = 27.2 eV) are used.

G is obtained from Dyson's equation

$$G = G^{\text{DFT}} + G^{\text{DFT}} [\Sigma_{\text{XC}} - v_{\text{XC}}] G, \quad (3)$$

where v_{XC} is the exchange and correlation DFT potential and Σ_{XC} is the *GW* electron self-energy.

Equation (3) is solved using a recent method developed to perform *GW* calculations in infinite, non-periodic geometries¹⁹ based on the embedding method.²⁰ The advantage of this approach is that the semi-infinite substrate, surface and vacuum regions are treated equally without the need for any fitting parameters or a repeated cell geometry.

The main steps of the computation are as follows: (i) The Kohn-Sham equation²¹ is solved self-consistently within LDA.²² In this framework, the embedding method permits an exact treatment of the semi-infinite substrate.

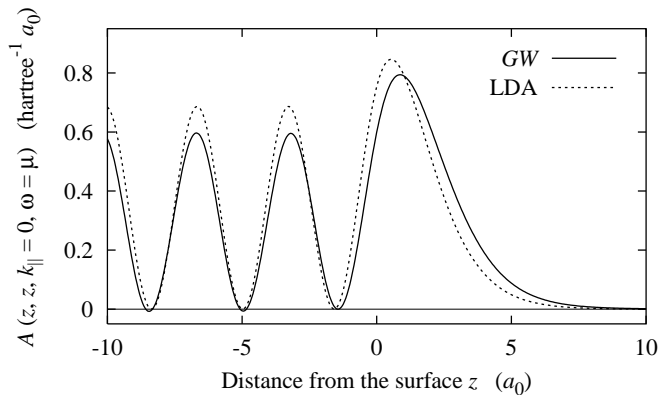


FIG. 1: Spectral weight function at the chemical potential and zero parallel wave-vector for semi-infinite jellium with $r_s = 2.07 a_0$.

G^{DFT} , obtained by numerical inversion of the Kohn-Sham Hamiltonian, describes a continuous spectrum of fictitious non-interacting electrons. (ii) From G^{DFT} we compute the polarization P in the random phase approximation. (iii) The inverse dielectric response, $(1 - vP)^{-1}$, yields the effective interaction W^{RPA} . (iv) The self-energy $\Sigma_{\text{XC}} = iG^{\text{DFT}}W^{\text{RPA}}$ is calculated using a real-space, imaginary-frequency representation and one obtains the self-energy on the real frequency axis by means of analytic continuation. (v) Equation (3) can now be solved to update G .

In Sec. II we present and discuss the results. Section III is devoted to conclusions.

II. RESULTS AND DISCUSSION

We examine first the z -dependence of the spectral weight function $A(z, \mathbf{k}_{\parallel}, \omega)$. This quantity is proportional to the probability amplitude for a particular wave-vector \mathbf{k}_{\parallel} and energy ω . In Fig. 1 we report $A(z, \mathbf{k}_{\parallel}, \omega)$ for k_{\parallel} equal to zero and ω equal to the chemical potential μ . All results shown in this Article are obtained for a jellium substrate of aluminum density ($r_s = 2.07 a_0$). The spectral weight outside the surface is enhanced by the improved description of exchange-correlation effects in GW , in common with the states of Al(111) studied in Ref. 23. By varying the energy ω we have verified that this feature is common to all bound states. In the bulk, the GW spectral weight is lower than that calculated by the LDA because some weight is transferred to lower energies through electron-plasmon coupling. The larger amplitude of A in the surface layer, together with the absence of decay into the bulk, identifies the states in this part of the surface band structure as forming a surface resonance.

In Fig. 2 we plot $\Delta\sigma = \sigma^{\text{GW}} - \sigma^{\text{LDA}}$, the difference between our many-body LDOS and that in the LDA. The energy-dependence of $\Delta\sigma$ as z moves from the bulk towards the vacuum is indicated by contour levels. We

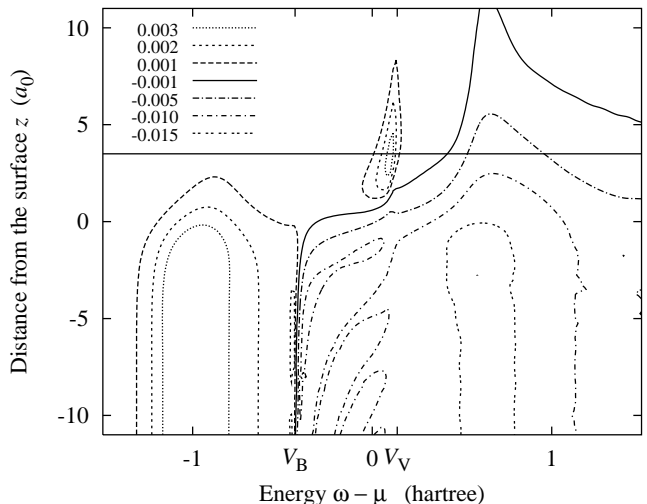


FIG. 2: Contour levels of $\Delta\sigma(z, \omega)$ for semi-infinite jellium with $r_s = 2.07 a_0$. The solid horizontal line indicates $z = 3.5 a_0$ (see Fig. 4). The pronounced “teardrop” feature at $z \sim 3.5 a_0$ is the surface image resonance. V_V is the vacuum energy level, and V_B the bottom of the free-electron band.

recapitulate that, for a jellium surface, the LDA effective potential $v_{\text{eff}}(z)$ approaches the constant limits V_B and V_V for $z \rightarrow -\infty$ (bulk) and $z \rightarrow +\infty$ (vacuum) respectively. As a consequence, the bulk and vacuum limits of σ^{LDA} are simply proportional to the well-known expressions $\sqrt{\omega - V_B}$ and $\sqrt{\omega - V_V}$. In the bulk, the LDA therefore predicts no states below V_B . The electron-plasmon coupling, automatically included in GW , is responsible for moving states down in energy from above to below V_B , yielding the sub-band shown in Fig. 3 for energies around 1 hartree below the chemical potential, as already demonstrated for the homogeneous electron gas.¹⁵

The presence of the surface is still noticeable even some atomic units into the substrate through Friedel oscillations, which are visible for bound energies from the contour levels of Fig. 2 and in the LDOS at a distance from the surface $z = -10 a_0$ in Fig. 3.

When z approaches the surface, coupling with plasmons considerably reduces, eventually becoming negligible a few atomic units outside the surface. As z moves into the vacuum, the electron density decays to zero. Self-energy effects are no longer present and the LDA description becomes exact. We then obtain $\Delta\sigma = 0$.

Apart from surface-truncated bulk structures, Fig. 2 also highlights a completely new feature in the form of a teardrop-shaped enhancement of the LDOS, localized in the near-surface region at energies between the chemical potential and the vacuum level. To highlight this feature we plot the energy dependence of $\Delta\sigma$ for $z = 3.5 a_0$ in Fig. 4 (note that this corresponds to a cross section plot along a horizontal line through Fig. 2). The peak in $\Delta\sigma$, located at about $1/32$ hartree below the vacuum

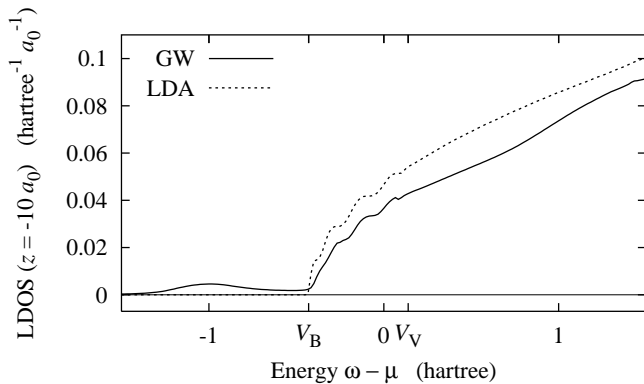


FIG. 3: LDOS σ^{GW} and σ^{LDA} for semi-infinite jellium with $r_s = 2.07 a_0$ at $z = -10 a_0$ from the jellium edge. The “ripples” between V_V and V_B indicate the presence of Friedel oscillations.

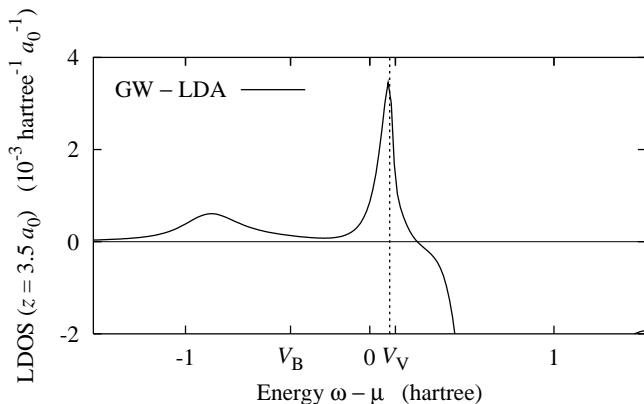


FIG. 4: Difference in the LDOS $\Delta\sigma$ for semi-infinite jellium with $r_s = 2.07 a_0$ at $z = 3.5 a_0$ from the surface. The dashed vertical line indicates the position of the first Rydberg state, $1/32$ hartree below the vacuum level.

level (the position of the first Rydberg state¹¹), clearly identifies an IPI surface resonance.

The presence of IPI resonances, even in the limiting case of a substrate without bulk reflectivity (the bulk reflectivity is associated with scattering by the atomic-cores²⁴), has been unclear. Simple model potentials in independent-particle approximations produced IPI resonances for jellium substrates²⁵ in some cases, but the presence of a clear resonance depended sensitively on the precise details of the chosen model. We remind that IPI states and resonances are a many-body phenomenon and can thus be included only in an *ad hoc* way in single-particle dynamic approximations. In contrast to these earlier, parameter-dependent results, our method is fully *ab initio* and includes many-body correlations.

In the case of semi-infinite jellium, the zero bulk reflectivity yields a large linewidth of the resonance, since hybridization with bulk states is not prevented at all. We estimate of the full width at half maximum (FWHM)

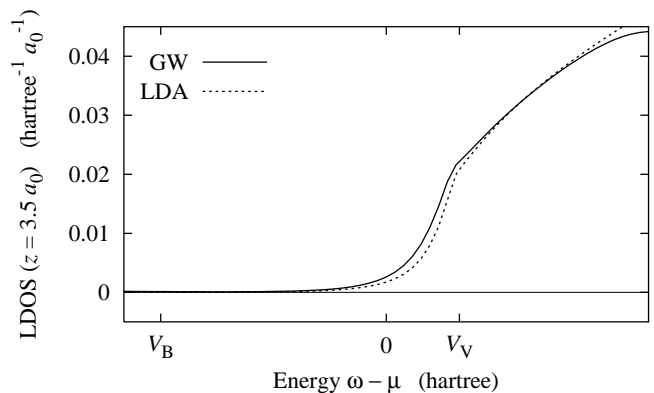


FIG. 5: Local density of states for a semi-infinite jellium with $r_s = 2.07 a_0$ at $z = 3.5 a_0$. The quantity reported in Fig. 4 is the difference between the continuous and the dashed line.

from $\Delta\sigma$ as 0.07 hartree (about 2 eV).²⁸ We remark that in systems without a bulk band gap the hybridization with the continuous bulk band is the major contributor to the linewidth, as the self-energy alone accounts only for about one tenth of the total FWHM.¹⁴

Owing to its large linewidth, the resonance shown in Fig. 4 encompasses the whole series of Rydberg image states,⁸ which in the infinite bulk barrier model extends from $V_V - 1/32$ hartree to V_V . The resonance is clearly visible in the difference plot between the many-body LDOS and the LDOS in the LDA. In the many-body LDOS itself, on the other hand, it resolves as a shoulder feature just below the vacuum energy (Fig. 5) rather than a distinct peak, because the LDA LDOS is already a strongly increasing function of energy in this range. The quantity reported in Fig. 4 is the difference between two theoretical quantities and is therefore not directly accessible to experiment. However, it allows us to isolate an important contribution to the phenomenon – the many-body interaction – which could improve the description of the electronic structure of real semi-infinite surfaces beyond the usual single-particle approaches such as Ref. 26.

We will now examine the origin of the resonance emerging in Fig. 4. For this reason it is important to look at the spectral weight function A , whose integral over \mathbf{k}_{\parallel} is the LDOS [Eq. (1)]. In Fig. 6 we present the energy dependence of $A(z, \mathbf{k}_{\parallel}, \omega)$ for $\mathbf{k}_{\parallel} = 0$ at the same position outside the jellium edge as Figs. 4 and 5 ($z = 3.5 a_0$).

We first consider the LDA result. For non-interacting particles in a constant potential V the z -resolved spectral weight function is essentially one-dimensional and hence proportional to $(\omega - k_{\parallel}^2/2 - V)^{-1/2}$. Thus in the vacuum a singularity is present at V_V for $k_{\parallel} = 0$. The spectral weight then diminishes with increasing energy. But near the surface weight is transferred to bulk states decaying out into the vacuum: the spectral function has a peak very close to $v_{\text{eff}}(z)$, but singularities are no longer present. We emphasize that in a slab geometry Fig. 6 would appear as a collection of delta functions, each delta corresponding to one of the discrete eigenstates.

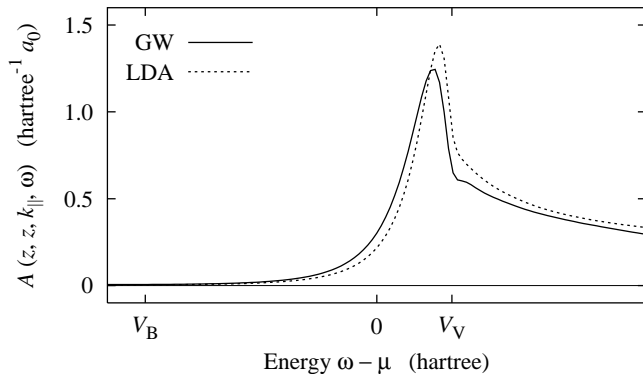


FIG. 6: Spectral weight function for a semi-infinite jellium with $r_s = 2.07 a_0$, for $k_{\parallel} = 0$ and $z = 3.5 a_0$. The integral over k_{\parallel} of this function gives the LDOS reported in Fig. 5.

When we describe the system in the interacting picture (*GW*), we still observe bulk states that spill out into the vacuum. But we also have a new class of states, constituting the IPI resonance. They have substantial weight at and outside the surface. As a consequence spectral weight from the LDA states is transferred into these quasiparticle states. Spectral weight hence moves down from higher energies to the energies of the IPI resonance. This produces the shoulder in A at V_V , and the displacement of the peak energy to lower energies.

If k_{\parallel} is increased from its zero value, the profile of A shown in Fig. 6 is shifted towards higher energies by $k_{\parallel}^2/2$, without being distorted too much (i.e., the dispersion of the states is nearly parabolic with effective mass equal

to 1). When we integrate over k_{\parallel} to get the LDOS, one notices that for energies roughly below V_V the *GW* spectral weight A^{GW} is greater than A^{LDA} for any value of k_{\parallel} , leading to the positive $\Delta\sigma$ shown in Fig. 4. For higher energies, $A^{GW} - A^{LDA}$ changes from negative to positive as k_{\parallel} increases. Negative contributions dominate and the corresponding $\Delta\sigma$ is negative.

III. CONCLUSIONS

In summary, we have evaluated from first principles the local density of states of a semi-infinite simple metal surface. Many-body correlations are included via the *GW* self-energy. The substrate is described as truly semi-infinite, thus enabling a calculation of the continuous spectrum necessary to properly account for the hybridization between surface electronic states and bulk states. We demonstrate the presence of an IPI resonance just below the vacuum energy, encompassing the full series of image-states that would be present in a system with a surface bandgap. The origin of the resonance is explained in terms of the spectral weight transfer to lower energies due to the inclusion of electron-electron correlation.

Acknowledgments

We are grateful to S. Modesti, L. G. Molinari, G. Onida, and M. I. Trioni for useful discussions. This work was supported by the Italian MIUR through Grant No. 2001021128. Patrick Rinke acknowledges the support of EPSRC and the DAAD.

* Present address: SISSA/ISAS, via Beirut 4, 34014 Trieste, Italy.

† Present address: Fritz-Haber-Institut der Max-Planck-Gesellschaft, Faradayweg 4–6, 14195 Berlin-Dahlem, Germany

¹ R. Matzdorf, *Surf. Sci. Repts.* **30**, 153 (1998).

² S. Schintke, S. Messerli, M. Pivetta, F. Patthey, L. Libioulle, M. Stengel, A. D. Vita, and W.-D. Schneider, *Phys. Rev. Lett.* **87**, 276801 (2001).

³ V. Dose, W. Altmann, A. Goldmann, U. Kolak, and J. Rogozik, *Phys. Rev. Lett.* **52**, 1919 (1984).

⁴ D. Straub and F. J. Himpsel, *Phys. Rev. Lett.* **52**, 1922 (1984).

⁵ K. Giesen, F. Hage, F. J. Himpsel, H. J. Riess, and W. Steinmann, *Phys. Rev. Lett.* **55**, 300 (1985).

⁶ T. Hertel, E. Knoesel, M. Wolf, and G. Ertl, *Phys. Rev. Lett.* **76**, 535 (1996).

⁷ D. Straub and F. J. Himpsel, *Phys. Rev. B* **33**, 2256 (1986).

⁸ B. Quiniou, V. Bulvović, and R. M. Osgood, *Phys. Rev. B* **47**, 15890 (1993).

⁹ S. Yang, R. A. Bartynski, G. P. Kochanski, S. Papadia, T. Fondén, and M. Persson, *Phys. Rev. Lett.* **70**, 849 (1993).

¹⁰ L. Petaccia, L. Grill, M. Zangrando, and S. Modesti, *Phys. Rev. Lett.* **82**, 386 (1999).

¹¹ P. M. Echenique and J. B. Pendry, *J. Phys. C: Solid State Phys.* **11**, 2065 (1978).

¹² P. M. Echenique, F. Flores, and F. Sols, *Phys. Rev. Lett.* **55**, 2348 (1985).

¹³ J. Bausells and P. M. Echenique, *Phys. Rev. B* **33**, 1471 (1986).

¹⁴ E. V. Chulkov, I. Sarría, V. M. Silkin, J. M. Pitarke, and P. M. Echenique, *Phys. Rev. Lett.* **80**, 4947 (1998).

¹⁵ L. Hedin and S. Lundqvist, *Solid State Physics*, vol. 23 (Academic Press, 1969).

¹⁶ A. G. Eguiluz, M. Heinrichsmeier, A. Fleszar, and W. Hanke, *Phys. Rev. Lett.* **68**, 1359 (1992).

¹⁷ J. J. Deisz, A. G. Eguiluz, and W. Hanke, *Phys. Rev. Lett.* **71**, 2793 (1993).

¹⁸ M. Heinrichsmeier, A. Fleszar, W. Hanke, and A. G. Eguiluz, *Phys. Rev. B* **57**, 14974 (1998).

¹⁹ G. Fratesi, G. P. Brivio, and L. G. Molinari, *cond-mat/0305344* (unpublished).

²⁰ J. E. Inglesfield, *J. Phys. C: Solid State Phys.* **14**, 3795 (1981).

²¹ W. Kohn and L. J. Sham, *Phys. Rev.* **140**, A1133 (1965).

- ²² J. P. Perdew and A. Zunger, Phys. Rev. B **23**, 5048 (1981).
- ²³ I. D. White, R. W. Godby, M. M. Rieger, and R. J. Needs, Phys. Rev. Lett. **80**, 4265 (1998).
- ²⁴ S. Papadia, M. Persson, and L.-A. Salmi, Phys. Rev. B **41**, 10237 (1990).
- ²⁵ S. A. Lindgren and L. Walldén, Phys. Rev. B **40**, 11546 (1989).
- ²⁶ H. Ishida, Phys. Rev. B **63**, 165409 (2001).
- ²⁷ V. Bulović, B. Quiniou, and R. M. Osgood, J. Vac. Sci. Technol. A **12**, 2201 (1994).
- ²⁸ Experimentally, the FWHMs of surface resonances at metal surfaces are usually of the order of tenths of eV.^{8,27} The difference may be explained by the non-negligible reflectivity of the atomic cores, reducing the hybridization with the underlying bulk continuum of states and thus the FWHM.